Kinematic models of the upper limb joints for multibody kinematics optimisation: An overview

Sonia Duprey, Alexandre Naaim, Florent Moissenet, Mickaël Begon, Laurence Cheze

Kinematic models of the upper limb joints for multibody kinematic optimisation:

an overview

Sonia Duprey[1*], Alexandre Naaim[2], Florent Moissenet[2], Mickaël Begon[3], Laurence Chèze[1]

[1] Univ Lyon, Université Claude Bernard Lyon 1, IFSTTAR, LBMC UMR_T9406, F69622, Lyon, France

[2] CNRFR – Rehazenter, Laboratoire d'Analyse du Mouvement et de la Posture, 1 rue André Vésale, L-2674 Luxembourg, Luxembourg

[3] Laboratoire de simulation et de modélisation du mouvement, Département de kinésiologie, Université de Montréal, 1700, rue Jacques Tétreault, Laval, QC H7N 0B6, Canada
Research Center, Sainte-Justine Hospital, 3175 Côte-Ste-Catherine, Montreal, Quebec, Canada H3T 1C5

*Corresponding author:
Sonia DUPREY
Laboratoire de Biomécanique et Mécanique des Chocs (LBMC)
IFSTTAR, Cité des Mobilités
25 Av F Mitterrand
69675 BRON Cedex
FRANCE
Phone: +33 (0)4 78 65 68 82
Email : sonia.duprey@univ-lyon1.fr

Orginial Article - Word Count : 3498 words

Abstract

Soft tissue artefact (STA), *i.e.* the motion of the skin, fat and muscles gliding on the underlying bone, may lead to a marker position error reaching up to 8.7 cm for the particular case of the scapula. Multibody kinematic optimisation (MBO) is one of the most efficient approaches used to reduce STA. It consists in minimising the distance between the positions of experimental markers on a subject skin and the simulated positions of the same markers embedded on a kinematic model. However, the efficiency of MBO directly relies on the chosen kinematic model. This paper proposes an overview of the different upper limb models available in the literature and a discussion about their applicability to MBO.

The advantages of each joint model with respect to its biofidelity to functional anatomy are detailed both for the shoulder and the forearm areas. Models capabilities of personalisation and of adaptation to pathological cases are also discussed. Concerning model efficiency in terms of STA reduction in MBO algorithms, a lack of quantitative assessment in the literature is noted. In priority, future studies should concern the evaluation and quantification of STA reduction depending on upper limb joint constraints.

Keywords: Multibody kinematic optimisation; Upper limb; Shoulder; Forearm; Kinematic model

1. Introduction

An accurate estimate of the upper limb kinematics is essential for ergonomic and clinical applications such as the prediction of the "reachable space" or the assessment of potential pathologies or lesions during arm elevations. However, estimating the skeleton kinematics from sensors or markers put on the skin is not trivial due to the soft tissue artefact (STA), *i.e.* the motion of the skin, fat and muscles gliding on the underlying bone. STA on the upper limb can be up to 8.7 cm on the scapula (Matsui et al., 2006) and up to 48% of the effective humeral axial rotation performed for the humerus (Cutti et al., 2005).

To reduce STA, both experimental and numerical approaches have been developed. Experimentally, the acromial part of the scapula (Leboeuf et al., 2012) and epicondyles of the humerus (Begon et al., 2015; Blache et al., 2016) are known to minimise STA. As for numerical approaches, some correction factors were determined (Bourne et al., 2009), but most of the studies relied on optimisation approaches. For instance, multibody kinematic optimisation (MBO) method is increasingly used since the first application of the Lu and O'Connor (1999) algorithm to the upper-limb by Roux et al. (2002). MBO consists in minimising the distance between the positions of experimental markers on the participant's skin and the estimated positions of the associated markers on a kinematic chain model. Optimisation performed on a single anatomical segment, called single-body optimisation (Cheze et al., 1995; Söderkvist and Wedin, 1993; Spoor and Veldpaus, 1980), might be ineffective. Indeed, it only correct marker cluster deformation while STA is mainly composed of cluster rigid transformations (Barré et al., 2013). Thus, compared to single-body optimisation, MBO should be more effective and non-physiological apparent joint dislocations should be avoided.

In the process of bone kinematic estimation through MBO, the choice of the upper limb joint models is decisive: MBO accuracy directly relies on the chosen joint constraints and degrees-of-freedom (DoF) (Duprey et al., 2010; Valente et al., 2015; Clément et al., 2014). Joint models should derive from actual functional anatomy. Several upper limb kinematic models are already available in the literature (see reviews by Yang et al. (2010), Dumas et al. (2016) and Tondu (2007)) and their number is expanding. Favre et al. (2009) highlighted an increasing interest in shoulder modelling: 30 publications from 1990 to 2009 *versus* more than 60 from 2000 to 2009. In the past 6 years, about 15 articles get published on shoulder modelling, confirming this interest.

3

Thus, the aim of this study was to provide an overview of the existing upper limb kinematic. Each model is discussed with respect to its biofidelity to functional anatomy, its capabilities of personalisation and adaptation to pathological cases, as well as its efficiency in terms of STA reduction in MBO algorithms.

2. Overview of the upper limb models

This overview is based on an extensive search in the Embase, Medline, Scopus, PubMed, and Web of Science databases with several combinations of the following keywords in the title, abstract or keywords: 'optim* *or* kalman', 'kinemat* joint', 'subject *or* human *or* limb', 'model* *or* over*determ*' and 'upper-limb *or* shoulder *or* elbow *or* wrist *or* *arm', and their references were searched for relevant upper limb kinematic models to be added.

Functional anatomy and existing kinematic models will be described and assessed, first for the shoulder and then for the forearm. All found models are sorted in Tables 1-2 according to their joint description. Only examples for each model category are cited in the following sections.

2.1. Shoulder

a) Functional anatomy

The shoulder is composed of three bones, the humerus, scapula and clavicle, and of four joints, the glenohumeral, sternoclavicular, acromioclavicular and the scapulathoracic joints (Figure 1). The glenohumeral joint is made of two spherical contact surfaces: the glenoid cavity and the humeral head connecting the scapula to the humerus. This results in a three DoFs rotation joint over a large range of motion (*i.e.* abduction 150-180°, flexion 180°, extension 45-60° and internal-external rotation 90°) with interaction between the DoFs as shown by Haering et al. (2014). Since both contact surfaces have different radii (*e.g.* a 1.3 mm difference was found in El Habachi et al. (2015)), the joint motion has also been described as "the movement of a ball on a seal nose" (Hill et al., 2008) implying a combination of large rotations and millimetre translations. Glenohumeral translations up to 12.4 mm were measured through *in vivo* studies (Dal Maso et al., 2014; Graichen et al., 2000; Sahara et al., 2007).

The sternoclavicular joint connects the clavicle to the thorax. In spite of its 2-DoF saddle-shaped joint nature, Zatsiorsky (1998, p348) emphasised this joint behaves as a ball-and-socket joint with three DoFs. The acromioclavicular joint links the acromion of the scapula to the lateral part of the clavicle. It allows a

rotation of the scapula about a specific screw axis passing through the insertions of both the acromioclavicular and the coracoclavicular ligaments with negligible translations (Sahara et al., 2006). The scapulothoracic joint does not include any articular structure, the gliding movement of the scapula on the thorax being only constrained by the surrounding muscles.

b) Modelling

Shoulder models account for previously described functional anatomy using series of kinematic constraints. The glenohumeral joint (or the shoulder as a whole) is commonly modelled as a spherical joint. To consider glenohumeral translations, some studies proposed a 6-DoF joint (Roux et al., 2002; van den Bogert et al., 2013) where soft constraints using a penalty-based method may be added (Charbonnier et al., 2014). In a different way, El Habachi et al. (2015) considered two spheres of different radii, one rolling on the another, to represent the glenoid cavity and humeral head interactions with possible translations (Figure 2). This constraint was modelled as a rod connecting the two sphere centres. Finally, a recent study suggested to model the glenohumeral joint as a simplified 2D cam-follower mechanism in order to predict shoulder instability using surface geometries and contact forces as inputs (Willemot et al., 2015).

The shoulder girdle can be represented as a single equivalent mechanism between the thorax and the glenohumeral joint. Different models of the shoulder girdle have been proposed namely a single universal joint, two prismatic joints, a universal joint with a prismatic joint or a parallel mechanism (Figure 3). Contrariwise, detailed representations of the shoulder girdle integrate the sternoclavicular and acromioclavicular joints separately.

The above modelling choices result in open-loop kinematic models, while models including a scapulothoracic joint result in a closed-loop chain. The combined motions of the clavicle and scapula relative to the thorax are constrained by the sternoclavicular, acromioclavicular and scapulothoracic joints (Figure 4). The scapulothoracic joint is commonly described as a contact between a cone or an ellipsoid representing the thorax and different points of the scapula. Recently, an equivalent but simpler mechanism made of two universal and two prismatic joints was proposed (Ingram et al., 2016). Finally, another way to integrate the interdependency between shoulder girdle DoFs is to introduce scapular and clavicular rhythm equations as a function of the humeral angles (de Groot and Brand, 2001).

5

c) *Assessment of the modelling choices*

Modelling the glenohumeral joint as a spherical joint is controversial. Glenohumeral translations are often considered as negligible since they are mostly under 5 mm for healthy subjects, however they might be up to 12.4 mm in maximum abduction (Dal Maso et al., 2014). Furthermore, in a clinical context, excessive translations may be related to shoulder disorders (Willemot et al., 2015) and have to be estimated to better understand the pathomechanics. Thus, depending on the application and the need for translation estimations, the glenohumeral joint can be set either as a spherical joint or include translations. For models dedicated to MBO, the use of a 6-DoF (no constraint) glenohumeral joint model would be a misuse of the method since MBO relies on physiological constraints to minimise the STA-related errors. Thus, for MBO purposes, models including limited translations seem to be an appropriate choice (Charbonnier et al., 2014; El Habachi et al., 2015), even though the "soft constraints" method raises the question of the weightings in the MBO cost function, since these factors controlling the amount of possible joint translations may be task or subject-dependent.

The acromioclavicular and sternoclavicular joints are mostly modelled as spherical joints. This modelling choice is satisfying since these DoFs may replicate kinematic observations. Furthermore, this choice enables the axial rotation of the clavicle which appears to play an important role in upper-extremity elevation since it may help to draw out the ligaments closing the acromioclavicular joint (Yang et al., 2010). However, clavicle axial rotation can hardly be measured due to STA, which raises the question of the legitimacy of modelling this clavicle DoF. Furthermore, most of the experimental studies do not attempt to measure this DoF (de Groot and Brand, 2001), while some try to assess axial rotation through optimisations either by minimising the acromioclavicular rotations (van der Helm and Pronk, 1995) or by constraining the conoid ligament to a constant length (Bolsterlee et al., 2013). To the best of our knowledge, only Sahara et al. (2006) and (Jackson et al., 2012a) provided 3D acromioclavicular and sternoclavicular kinematics during arm elevations, using either MRI data or several cutaneous markers on the clavicle, respectively. A partial solution could be to add bounds based on these experimental observations.

The modelling choice of the scapulothoracic joint which consists in defining contact points of the scapula on an ellipsoid representing the thorax is widespread. However, there is no consensus on the number and location of the contact points. The ellipsoid construction also depends on the study (scaled or optimised shapes). Furthermore, this method can lead to non-physiological interpenetrations of the scapula into the thorax. Solutions to this problem have been proposed in the literature by imposing the scapula plane to be

tangential to different geometries representing the thorax (Naaim et al., 2015; Tondu, 2007) or by introducing an equivalent parallel mechanism made of universal and prismatic joints (Ingram et al., 2016) that may be simpler to implement than the gliding conditions. These last models have the advantages of being easily customisable to patients.

The approach relying on a set shoulder rhythm (*i.e.* coupling equations of sternoclavicular, acromioclavicular and glenohumeral joint angles as function of the thoracohumeral elevation) is easy to implement, nevertheless these equations are based on measurements performed on relatively small and homogeneous samples of healthy subjects and selected movements (de Groot and Brand, 2001; Grewal and Dickerson, 2013). Thus, models integrating such regressions might fail to represent independent scapula and humerus motions like shrugging and will not allow to discriminate between normal and pathological scapular kinematics.

2.2. Forearm

a) *Functional anatomy*

The forearm is composed of two bones, the radius and ulna that interact together proximally with the humerus and distally with the hand through five joints, the humeroulnar, the humeroradial, the proximal and distal radioulnar, and the wrist or radiocarpal joints (Figure 5).

The humeroulnar joint consists in the contact between the humeral trochlea and the trochlear notch of the ulna. This joint allows three DoFs. The primary DoF corresponds to the flexion-extension with up to 160° of passive flexion. For that, the humeral trochlea has a diabolo shape and the trochlear notch of the ulna presents a high congruence to this shape. This prevents any medial-lateral displacements and thus ensures the stability of the joint. It must be noticed that the trochlea extends more distally than the capitulum, leading to an angulation called carrying angle observed between the longitudinal axes of the humerus and the forearm. Additionally, during pronosupination, the ulna describes an arc of circle composed of an extension followed by a lateral motion and finally a flexion relative to the humerus (Duchenne, 1959; Dwight, 1885). Two additional DoFs are thus observed: an ulna axial displacement and a humeroulnar abduction-adduction movement (*i.e.* swaying) (Gattamelata et al., 2007).

The humeroradial joint connects the humerus capitulum to the radial head. While the bony surfaces of this joint enable three rotational DoFs, a second contact between the radial head and the ulnar radial notch prevents instability and limits the movement to almost a unique DoF in flexion-extension. The latter contact,

ensured by the annular ligament, corresponds to the proximal radioulnar joint. The combination of proximal and distal radioulnar joints allows the pronosupination. This additional rotational DoF ensures an accurate positioning of the hand which is connected to the distal end of the radius through the radiocarpal joint.

The articular surface of the radius forms a transversely elliptical concave surface that can receive the smooth convex surface of the condyle formed by the superior articular surfaces of the carpal bones, specifically the navicular, lunate, and triangular bones (*i.e.* radiocarpal joint). The movements permitted by this joint are flexion-extension and abduction-adduction.

b) *Modelling*

In biomechanics, the forearm is commonly considered as a single segment. The elbow and the wrist are modelled as universal joints where the pronosupination is often reported at the elbow. For instance, Prokopenko et al. (2001) integrated non-orthogonal and non-intersecting axes in the elbow and wrist joints in their open-loop arm model in order to respect anatomical considerations.

When a more detailed model of the forearm is required, the main challenge is to reproduce the pronosupination in an anatomical manner. Introduced by Fick as early as 1904 (cited in Fick, 2013), a first level of modelling integrating pronosupination consists in two L-shaped elements connected by two spherical joints representing the humeroradial and distal radioulnar joints. This model leads to an unrealistic adduction movement of the hand since the parallelism between elbow and wrist flexion-extension axis cannot be conserved during pronosupination. To remove this limitation, some authors proposed to add a translational DoF between radius and ulna, at the proximal radioulnar (Pennestrì et al., 2007; Weinberg et al., 2000) or at the distal radioulnar joint (Lemay and Crago, 1996). In the model of Lemay and Cargo (1996), the distal radioulnar joint was modelled as a cylindrical joint along the axis going through the capitulum and the centre of the distal part of the ulna. Weinberg et al (2000) proposed another closed-loop kinematic chain enabling to reproduce the anatomical evasive motion between ulna and radius. The proximal radioulnar joint was a spherical joint (at the ulna proximal end) rigidly linked to a prismatic joint (at the radius proximal end), and the distal radioulnar joint was a hinge joint (at the ulna distal end) rigidly linked to a universal joint (at the radius distal end). Pennestri et al (2007) proposed a similar mechanism where the universal joint was replaced by a spherical joint and the prismatic joint by a guide joint (Figure 6).

To reproduce the ulna axial displacement and the swaying observed *in vivo* (Gattamelata et al., 2007), further DoFs may be introduced into the humeroulnar joint, namely a translation in the direction of the hinge

axis and a rotation for humeroulnar abduction-adduction. Moreover, the carrying angle is rarely reported in the models. To fill these gaps, Laitenberger et al. (2014) proposed a complete model of the upper limb, integrating a closed-loop forearm model. The forearm part of this model was composed of the humeroulnar joint (hinge joint), the humeroradial joint (spherical joint), the proximal radioulnar joint (hinge joint coupled with a prismatic joint), and the distal radioulnar joint (three hinge joints).

c)   Assessment of the modelling choices

The open-loop models with universal joints at both the elbow and wrist can be a reasonable compromise between accuracy and simplicity of the human arm description (Prokopenko et al., 2001) for direct kinematics applications. For models dedicated to MBO, additional details are required to reproduce pronosupination in an anatomical manner and closed-loop models seem thus more appropriate (Laitenberger et al., 2014). However, as for the shoulder girdle, adding too many DoFs can be deleterious to the MBO approach as the STA-related errors are partially corrected through the kinematic constraints. Anyway, the models defining one DoF at the humeroulnar joint (Pennestrì et al., 2007) and one and two DoFs at the closed-loop associated to the radioulnar and humeroradial joints (Laitenberger et al., 2014) were both able to reproduce the complex movement of the forearm based on anatomical considerations.

In most of the forearm models, the focus is put on the pronosupination function of the forearm, leaving the humeroulnar joint to its primary function (*i.e.* flexion-extension) through the use of a hinge joint. However, the anatomy of this joint is more complex and allows further DoFs, as described previously. To the authors' knowledge, only Laitenberger et al. (2014) defined the humeroulnar joint by a universal joint (*i.e.* flexion-extension, abduction-adduction) coupled with a prismatic joint. Compared to other forearm models, this model demonstrated a better biofidelic reproduction of the movements between forearm bones.

3.   Discussion

The objective of the present overview was to describe existing upper limb models and discuss their applicability using MBO. This overview is based on an extensive search of several major databases. The large variability and inaccuracy of the expressions used to describe MBO (*e.g.* global optimisation, inverse kinematics, motion reconstruction, overdetermined system as previously highlighted by Dumas et al. (2016)) made a systematic review inappropriate. A search with specific keywords could fail finding relevant

9

articles, while a search with general keywords would lead to a very substantial number of articles. This overview manages to render the major trends concerning upper limb modelling in the goal of STA reduction. In all, 37 studies about upper limb modelling were found, with 38% of them used in MBO (Tables 1-2). While lower limb models are classically dedicated to gait analysis, there is no standard activity for the upper limb. Thus the models are built according to the purpose and the intended application. This may explain the variety of models found in the literature.

3.1 Personalisation of upper limb kinematic model

Each joint model was assessed by considering its biofidelity to functional anatomy. However, in the context of STA reduction, joint constraints do not only have to be anatomically biofidelic but also have to 1) be easily customisable to each participant including those with musculoskeletal disorders (Clément et al., 2016) and 2) to reduce STA. Subjects' anthropometry fitting can easily be performed by adjusting each segment length based on geometrical measurements for simple upper limb models. For more complex models, medical images might be needed, to adjust the humeral head and glenoid radii for instance (El Habachi et al., 2015), to find the ellipsoid best fitting the thorax (Prinold and Bull, 2014) or accurately locate joint centres (Michaud et al., 2016). This requirement is somehow a limitation since it can only be afforded in a clinical context. Adaptation of joint constraints to fit pathological cases is a complex step since it requires an a priori knowledge of the pathology in order to adequately reduce STA. In the case of pathologies leading to bone deformities or range of motions restrictions, joint models allowing to adapt joint surface geometries or allowing to tune the bounds of some DoFs, especially translations, are of interest. The approaches relying on coupling equations cannot account for pathologies.

3.2. Upper-limb MBO and STA reduction

In MBO framework, open-loop chain models including mostly universal and spherical joints present the advantage of avoiding non-physiological joint dislocation which appears when using single-body optimisation. In the context of clinical applications, more complex models may be needed for their higher biofidelity in terms of functional anatomy and their personalisation capabilities as mentioned above. However, in the literature, there is a lack of studies concerning the assessment of STA reduction through MBO for the upper limb: only a few studies (El Habachi et al., 2015; Charbonnier et al., 2014; Begon et al., n.d., Naaim et al., 2015) quantified the errors due to STA compared to experimental reference data. All but

Naaim et al. (n.d.) generally reported significant reductions of the STA. However, the lack of comparative studies investigating different upper limb joint constraints makes it difficult to conclusively determine the best joint kinematic constraints/models for STA reduction. Also, all segments and joints should be modelled since each constraint may affect all DoFs (Begon et al., n.d.). Another shortage of the literature is the lack of sensitivity studies enabling to assess the influence of the model parameters such as clavicle length, position of the scapulo-thoracic contact and of the thorax ellipsoid centre (El Habachi et al., 2013). Such studies are essential to identify the key parameters of a model.

3.3 Conclusion and future directions

A large number of upper limb models with a large variety of joint modelling choices was pointed out. Models as close as possible to functional anatomy appear to be attractive: they can be adapted to pathological cases and a better STA reduction is expected. Nevertheless, the influence of joint constraints on STA reduction appears to be little known. Thus, major future directions should concern the evaluation and quantification of STA reduction depending on joint constraints, as well as the determination, through sensitivity studies, of the most influent parameters in the upper limb models dedicated to MBO.

References

Abdel-Malek, K., Yang, J., Marler, T., Beck, S., Mathai, A., Zhou, X., Patrick, A., Arora, J., 2006. Towards a new generation of virtual humans. International Journal of Human Factors Modelling and Simulation 1, 2–39. doi:10.1504/IJHFMS.2006.011680

Barré, A., Thiran, J.P., Jolles, B.M., Theumann, N., Aminian, K., 2013. Soft Tissue Artifact Assessment During Treadmill Walking in Subjects With Total Knee Arthroplasty. IEEE Transactions on Biomedical Engineering 60, 3131–3140. doi:10.1109/TBME.2013.2268938

Begon, M., Bélaise, C., Naaim, A., Lundberg, A., Chèze, L., n.d. Multibody kinematic optimization with marker projection improves the accuracy of the humerus rotational kinematics. Journal of Biomechanics. doi:10.1016/j.jbiomech.2016.09.046

Begon, M., Dal Maso, F., Arndt, A., Monnet, T., 2015. Can optimal marker weightings improve thoracohumeral kinematics accuracy? Journal of Biomechanics 48, 2019–2025. doi:10.1016/j.jbiomech.2015.03.023

Berthonnaud, E., Herzberg, G., Morrow, D., An, K.-N., Dimnet, J., 2006. In vivo location of joint centers of the shoulder system: gleno-humeral and scapulo-thoracic joints between two postures describing the arm elevation in the plane of scapula using techniques based upon biplanar radiography. J. Mech. Med. Biol. 06, 385–397. doi:10.1142/S0219519406002060

Blache, Y., Dumas, R., Lundberg, A., Begon, M., 2016. Main component of soft tissue artifact of the upper-limbs with respect to different functional, daily life and sports movements. Journal of Biomechanics. doi:10.1016/j.jbiomech.2016.10.019

Blana, D., Hincapie, J.G., Chadwick, E.K., Kirsch, R.F., 2008. A musculoskeletal model of the upper extremity for use in the development of neuroprosthetic systems. Journal of Biomechanics 41, 1714–1721. doi:10.1016/j.jbiomech.2008.03.001

Bolsterlee, B., Veeger, H.E.J., Helm, F.C.T. van der, 2013. Modelling clavicular and scapular kinematics: from measurement to simulation. Med Biol Eng Comput 52, 283–291. doi:10.1007/s11517-013-1065-2

Bourne, D.A., Choo, A.M., Regan, W.D., MacIntyre, D.L., Oxland, T.R., 2009. A New Subject-Specific Skin Correction Factor for Three-Dimensional Kinematic Analysis of the Scapula. Journal of Biomechanical Engineering 131, 121009–121009. doi:10.1115/1.4000284

Cerveri, P., Pedotti, A., Ferrigno, G., 2003. Robust recovery of human motion from video using Kalman filters and virtual humans. Human Movement Science 22, 377–404. doi:10.1016/S0167-9457(03)00004-6

Charbonnier, C., Chagué, S., Kolo, F.C., Chow, J.C.K., Lädermann, A., 2014. A patient-specific measurement technique to model shoulder joint kinematics. Orthopaedics & Traumatology: Surgery & Research 100, 715–719. doi:10.1016/j.otsr.2014.06.015

Cheze, L., Fregly, B.J., Dimnet, J., 1995. A solidification procedure to facilitate kinematic analyses based on video system data. Journal of Biomechanics 28, 879–884. doi:10.1016/0021-9290(95)95278-D

Clément, J., Dumas, R., Hagemeister, N., Guise, J.A. de, 2016. Can generic knee joint models improve the measurement of osteoarthritic knee kinematics during squatting activity? Computer Methods in Biomechanics and Biomedical Engineering 0, 1–10. doi:10.1080/10255842.2016.1202935

Clément, J., Hagemeister, N., Dumas, R., Kanhonou, M., Guise, J.A. de, 2014. Influence of biomechanical multi-joint models used in global optimisation to estimate healthy and osteoarthritis knee kinematics. Computer Methods in Biomechanics and Biomedical Engineering 17, 76–77. doi:10.1080/10255842.2014.931141

Cutti, A.G., Paolini, G., Troncossi, M., Cappello, A., Davalli, A., 2005. Soft tissue artefact assessment in humeral axial rotation. Gait & Posture 21, 341–349. doi:10.1016/j.gaitpost.2004.04.001

Dal Maso, F., Raison, M., Lundberg, A., Arndt, A., Begon, M., 2014. Coupling between 3D displacements and rotations at the glenohumeral joint during dynamic tasks in healthy participants. Clinical Biomechanics 29, 1048–1055. doi:10.1016/j.clinbiomech.2014.08.006

de Groot, J.H., Brand, R., 2001. A three-dimensional regression model of the shoulder rhythm. Clinical Biomechanics 16, 735–743. doi:10.1016/S0268-0033(01)00065-1

Debril, J.-F., Pudlo, P., Simoneau, E., Gorce, P., Lepoutre, F.X., 2011. A method for calculating the joint coordinates of paraplegic subjects during the transfer movement despite the loss of reflective markers. International Journal of Industrial Ergonomics 41, 153–166. doi:10.1016/j.ergon.2010.12.003

Dickerson, C.R., Chaffin, D.B., Hughes, R.E., 2007. A mathematical musculoskeletal shoulder model for proactive ergonomic analysis. Computer Methods in Biomechanics and Biomedical Engineering 10, 389–400. doi:10.1080/10255840701592727

Dubowsky, S.R., Rasmussen, J., Sisto, S.A., Langrana, N.A., 2008. Validation of a musculoskeletal model of wheelchair propulsion and its application to minimizing shoulder joint forces. Journal of Biomechanics 41, 2981–2988. doi:10.1016/j.jbiomech.2008.07.032

Duchenne, G.B., 1959. Physiology of motion demonstrated by means of electrical stimulation and clinical observation and applied to the study of paralysis and deformities. WB Saunders., WB Saunders. ed.

12

Dumas, R., Andersen, M.S., Begon, M., 2016. What are the joint models used in multibody kinematic optimisation for the estimation of human joint kinematics? A review. Presented at the Digital Human Modelling, Montreal, Québec, Canada.

Duprey, S., Cheze, L., Dumas, R., 2010. Influence of joint constraints on lower limb kinematics estimation from skin markers using global optimization. Journal of Biomechanics 43, 2858–2862. doi:10.1016/j.jbiomech.2010.06.010

Dwight, T., 1885. The Movements of the Ulna in Rotation of the Fore-Arm. J Anat Physiol 19, 186–189.

El Habachi, A., Duprey, S., Cheze, L., Dumas, R., 2015. A parallel mechanism of the shoulder—application to multi-body optimisation. Multibody System Dynamics 33, 439–451.

El Habachi, A., Duprey, S., Cheze, L., Dumas, R., 2013. Global sensitivity analysis of the kinematics obtained with a multi-body optimisation using a parallel mechanism of the shoulder. Computer methods in biomechanics and biomedical engineering 16, 61–62.

Engin, A.E., Tümer, S.T., 1989. Three-Dimensional Kinematic Modelling of the Human Shoulder Complex—Part I: Physical Model and Determination of Joint Sinus Cones. J Biomech Eng 111, 107–112. doi:10.1115/1.3168351

Fick, R., 2013. Handbuch Der Anatomie und Mechanik Der Gelenke Unter Berücksichtigung Der Bewegenden Muskeln, BoD – Books on Demand. ed. BoD – Books on Demand.

Fohanno, V., Begon, M., Lacouture, P., Colloud, F., 2013. Estimating joint kinematics of a whole body chain model with closed-loop constraints. Multibody Syst Dyn 31, 433–449. doi:10.1007/s11044-013-9366-7

Garner, B.A., Pandy, M.G., 1999. A Kinematic Model of the Upper Limb Based on the Visible Human Project (VHP) Image Dataset. Computer Methods in Biomechanics and Biomedical Engineering 2, 107–124. doi:10.1080/10255849908907981

Gattamelata, D., Pezzuti, E., Valentini, P.P., 2007. Accurate geometrical constraints for the computer aided modelling of the human upper limb. Computer-Aided Design, Human Modeling and Applications 39, 540–547. doi:10.1016/j.cad.2007.01.009

Graichen, H., Stammberger, T., Bonel, H., Englmeier, K.-H., Reiser, M., Eckstein, F., 2000. Glenohumeral translation during active and passive elevation of the shoulder — a 3D open-MRI study. Journal of Biomechanics 33, 609–613. doi:10.1016/S0021-9290(99)00209-2

Haering, D., Raison, M., Begon, M., 2014. Measurement and Description of Three-Dimensional Shoulder Range of Motion With Degrees of Freedom Interactions. J Biomech Eng 136, 084502–084502. doi:10.1115/1.4027665

Hill, A.M., Bull, A.M.J., Wallace, A.L., Johnson, G.R., 2008. Qualitative and quantitative descriptions of glenohumeral motion. Gait & Posture 27, 177–188. doi:10.1016/j.gaitpost.2007.04.008

Högfors, C., Peterson, B., Sigholm, G., Herberts, P., 1991. Biomechanical model of the human shoulder joint—II. The shoulder rhythm. Journal of Biomechanics 24, 699–709. doi:10.1016/0021-9290(91)90334-J

Holzbaur, K.R.S., Murray, W.M., Delp, S.L., 2005. A Model of the Upper Extremity for Simulating Musculoskeletal Surgery and Analyzing Neuromuscular Control. Ann Biomed Eng 33, 829–840. doi:10.1007/s10439-005-3320-7

Ingram, D., Engelhardt, C., Farron, A., Terrier, A., Müllhaupt, P., 2016. Modelling of the human shoulder as a parallel mechanism without constraints. Mechanism and Machine Theory 100, 120–137. doi:10.1016/j.mechmachtheory.2016.02.004

Jackson, M., Michaud, B., Tétreault, P., Begon, M., 2012a. Improvements in measuring shoulder joint kinematics. Journal of Biomechanics 45, 2180–2183. doi:10.1016/j.jbiomech.2012.05.042

Jackson, M., Michaud, B., Tétreault, P., Begon, M., 2012b. Improvements in measuring shoulder joint kinematics. Journal of Biomechanics 45, 2180–2183. doi:10.1016/j.jbiomech.2012.05.042

Karlsson, D., Peterson, B., 1992. Towards a model for force predictions in the human shoulder. Journal of Biomechanics 25, 189–199. doi:10.1016/0021-9290(92)90275-6

Klopčar, N., Lenarčič, J., 2006. Bilateral and unilateral shoulder girdle kinematics during humeral elevation. Clinical Biomechanics, Proceedings of the 5th Meeting of the International Shoulder Group 21, Supplement 1, S20–S26. doi:10.1016/j.clinbiomech.2005.09.009

Laitenberger, M., Raison, M., Périé, D., Begon, M., 2014. Refinement of the upper limb joint kinematics and dynamics using a subject-specific closed-loop forearm model. Multibody Syst Dyn 33, 413–438. doi:10.1007/s11044-014-9421-z

Leboeuf, F., Schwartz, C., Brochard, S., Lempereur, M., Burdin, V., Remy-Neris, O., 2012. Relevance of skin deformation to track the scapula during forward humeral elevations. Computer Methods in Biomechanics and Biomedical Engineering 15, 365–367. doi:10.1080/10255842.2012.713694

Lemay, M.A., Crago, P.E., 1996. A dynamic model for simulating movements of the elbow, forearm, and wrist. Journal of Biomechanics 29, 1319–1330. doi:10.1016/0021-9290(96)00026-7

Lenarcic, J., Stanisic, M., 2003. A humanoid shoulder complex and the humeral pointing kinematics. IEEE Transactions on Robotics and Automation 19, 499–506. doi:10.1109/TRA.2003.810578

13

Lenarcic, J., Umek, A., 1994. Simple model of human arm reachable workspace. IEEE Transactions on Systems, Man, and Cybernetics 24, 1239–1246. doi:10.1109/21.299704

Lu, T.-W., O'Connor, J.J., 1999. Bone position estimation from skin marker co-ordinates using global optimisation with joint constraints. Journal of Biomechanics 32, 129–134. doi:10.1016/S0021-9290(98)00158-4

Matsui, K., Shimada, K., Andrew, P.D., 2006. Deviation of skin marker from bone target during movement of the scapula. Journal of Orthopaedic Science 11, 180–4.

Maurel, W., Thalmann, D., 1999. A Case Study on Human Upper Limb Modelling for Dynamic Simulation. Computer Methods in Biomechanics and Biomedical Engineering 2, 65–82. doi:10.1080/10255849908907979

Michaud, B., Jackson, M., Arndt, A., Lundberg, A., Begon, M., 2016. Determining in vivo sternoclavicular, acromioclavicular and glenohumeral joint centre locations from skin markers, CT-scans and intracortical pins: A comparison study. Medical Engineering & Physics 38, 290–296. doi:10.1016/j.medengphy.2015.12.004

Naaim, A., Moissenet, F., Dumas, R., Begon, M., Chèze, L., 2015. Comparison and validation of five scapulothoracic models for correcting soft tissue artefact through multibody optimisation. Computer Methods in Biomechanics and Biomedical Engineering 18, 2014–2015. doi:10.1080/10255842.2015.1069561

Naaim, A., Moissenet, F., Duprey, S., Begon, M., Chèze, L., n.d. Effect of various upper limb multibody models on soft tissue artefact correction: a case study. Journal of Biomechanics, Submitted in September 2016.

Pennestrì, E., Stefanelli, R., Valentini, P.P., Vita, L., 2007. Virtual musculo-skeletal model for the biomechanical analysis of the upper limb. Journal of Biomechanics 40, 1350–1361. doi:10.1016/j.jbiomech.2006.05.013

Pontonnier, C., Dumont, G., 2009. Inverse dynamics method using optimization techniques for the estimation of muscles forces involved in the elbow motion. Int J Interact Des Manuf 3, 227–236. doi:10.1007/s12008-009-0078-4

Prinold, J.A.I., Bull, A.M.J., 2014. Scaling and kinematics optimisation of the scapula and thorax in upper limb musculoskeletal models. Journal of Biomechanics 47, 2813–2819. doi:10.1016/j.jbiomech.2014.05.015

Prokopenko, R.A., Frolov, A.A., Biryukova, E.V., Roby-Brami, A., 2001. Assessment of the accuracy of a human arm model with seven degrees of freedom. Journal of Biomechanics 34, 177–185. doi:10.1016/S0021-9290(00)00179-2

Quental, C., Folgado, J., Ambrósio, J., Monteiro, J., 2012. A multibody biomechanical model of the upper limb including the shoulder girdle. Multibody Syst Dyn 28, 83–108. doi:10.1007/s11044-011-9297-0

Roux, E., Bouilland, S., Godillon-Maquinghen, A.-P., Bouttens, D., 2002. Evaluation of the global optimisation method within the upper limb kinematics analysis. Journal of Biomechanics 35, 1279–1283. doi:10.1016/S0021-9290(02)00088-X

Sahara, W., Sugamoto, K., Murai, M., Tanaka, H., Yoshikawa, H., 2007. The three-dimensional motions of glenohumeral joint under semi-loaded condition during arm abduction using vertically open MRI. Clinical Biomechanics 22, 304–312. doi:10.1016/j.clinbiomech.2006.04.012

Sahara, W., Sugamoto, K., Murai, M., Tanaka, H., Yoshikawa, H., 2006. 3D kinematic analysis of the acromioclavicular joint during arm abduction using vertically open MRI. J. Orthop. Res. 24, 1823–1831. doi:10.1002/jor.20208

Saul, K.R., Hu, X., Goehler, C.M., Vidt, M.E., Daly, M., Velisar, A., Murray, W.M., 2015. Benchmarking of dynamic simulation predictions in two software platforms using an upper limb musculoskeletal model. Computer Methods in Biomechanics and Biomedical Engineering 18, 1445–1458. doi:10.1080/10255842.2014.916698

Seth, A., Matias, R., Veloso, A.P., Delp, S.L., 2016. A Biomechanical Model of the Scapulothoracic Joint to Accurately Capture Scapular Kinematics during Shoulder Movements. PLOS ONE 11, e0141028. doi:10.1371/journal.pone.0141028

Sholukha, V., Bonnechere, B., Salvia, P., Moiseev, F., Rooze, M., Van Sint Jan, S., 2013. Model-based approach for human kinematics reconstruction from markerless and marker-based motion analysis systems. Journal of Biomechanics 46, 2363–2371. doi:10.1016/j.jbiomech.2013.07.037

Söderkvist, I., Wedin, P.-Å., 1993. Determining the movements of the skeleton using well-configured markers. Journal of Biomechanics 26, 1473–1477. doi:10.1016/0021-9290(93)90098-Y

Spoor, C.W., Veldpaus, F.E., 1980. Rigid body motion calculated from spatial co-ordinates of markers. Journal of Biomechanics 13, 391–393. doi:10.1016/0021-9290(80)90020-2

Tondu, B., 2007. Estimating shoulder-complex mobility. Applied Bionics and Biomechanics 4, 19–29. doi:10.1080/11762320701403922

14

van den Bogert, A.J., Geijtenbeek, T., Even-Zohar, O., Steenbrink, F., Hardin, E.C., 2013. A real-time system for biomechanical analysis of human movement and muscle function. Med Biol Eng Comput 51, 1069–1077. doi:10.1007/s11517-013-1076-z

van der Helm, F.C.T., 1994a. Analysis of the kinematic and dynamic behavior of the shoulder mechanism. Journal of Biomechanics 27, 527–550. doi:10.1016/0021-9290(94)90064-7

van der Helm, F.C.T., 1994b. A finite element musculoskeletal model of the shoulder mechanism. Journal of Biomechanics 27, 551–569. doi:10.1016/0021-9290(94)90065-5

van der Helm, F.C.T., Pronk, G.M., 1995. Three-Dimensional Recording and Description of Motions of the Shoulder Mechanism. J Biomech Eng 117, 27–40. doi:10.1115/1.2792267

Weinberg, A.M., Pietsch, I.T., Helm, M.B., Hesselbach, J., Tscherne, H., 2000. A new kinematic model of pro- and supination of the human forearm. Journal of Biomechanics 33, 487–491. doi:10.1016/S0021-9290(99)00195-5

Willemot, L., Thoreson, A., Breighner, R., Hooke, A., Verborgt, O., An, K.-N., 2015. Mid-range shoulder instability modeled as a cam-follower mechanism. Journal of Biomechanics 48, 2227–2231. doi:10.1016/j.jbiomech.2015.02.053

Yang, J., Abdel-Malek, K., Nebel, K., 2003. The Reach Envelope of a 9 Degree-of-Freedom Model of the Upper Extremity.

Yang, J., Feng, X., Kim, J.H., Rajulu, S., 2010. Review of biomechanical models for human shoulder complex. International Journal of Human Factors Modelling and Simulation 1, 271–293. doi:10.1504/IJHFMS.2010.036791

Zatsiorsky, V., 1998. Kinematics of Human Motion, Human Kinetics. ed. Champaign, IL, USA.
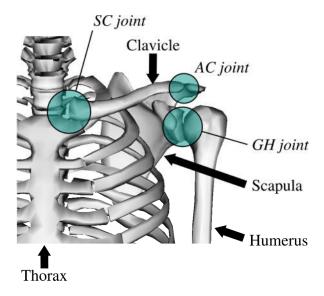
15

Figures
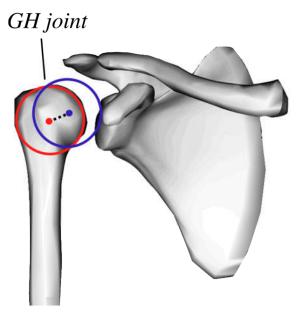

Figure 1: Shoulder girdle anatomy

Figure 2: Glenohumeral joint modelled as a sphere-to-sphere contact (El Habachi et al., 2015)
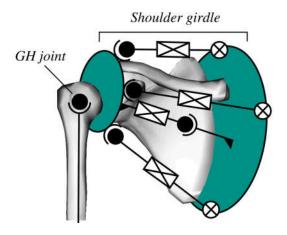
Figure 3: Shoulder girdle modelled as a parallel mechanism (Lenarcic and Stanisic, 2003)
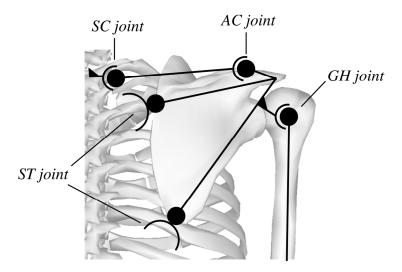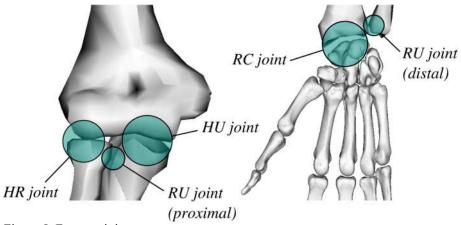

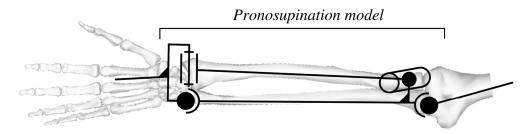Figure 4: A closed-loop kinematic chain of the shoulder

Figure 5: Forearm joints

Pronosupination model

Figure 6 : Forearm kinematic model as proposed by Pennestrì et al. (2007)

Tables

Table 1: Joint models of the shoulder (the MBO column indicates whether the model was initially built for multibody kinematic optimisation purposes)

Joints	Kinematics	References	Comments	MBO
Shoulder as a single joint	Spherical joint	Engin and Tümer, 1989		
		Prokopenko et al., 2001		x
		Cerveri et al., 2003		x
		Pontonnier and Dumont, 2009		x
		Debril et al., 2011		x
		Fohanno et al., 2013		x
GH joint	Spherical joint	Garner and Pandy, 1999		
		Högfors et al., 1991		
		Maurel and Thalmann, 1999		
		van der Helm, 1994		
		Yang et al., 2003		
	6 DoF	Roux et al., 2002		x
		van den Bogert et al., 2013		x
	Soft constraints	Charbonnier et al., 2014		x
	Sphere-to-sphere	El Habachi et al., 2015		x
	Cam-follower mechanism	Willemot et al., 2015	2D mechanism	
Shoulder girdle as a single mechanism	Universal joint	Lenarcic and Umek, 1994		
		Abdel-Malek et al., 2006		
	Two prismatic joints	Yang et al., 2003		
	Universal joint + Prismatic joint	Klopčar and Lenarčič, 2006		
	Parallel mechanism	Lenarcic and Stanisic, 2003		
AC and SC joints	Two spherical joints	Högfors et al., 1991		
		Yang et al., 2010		
		Jackson et al., 2012	Clavicle axial rotation allowed	x
		Charbonnier et al., 2014		x
		Laitenberger et al., 2014		x
ST joint	Cone or ellipsoid contact	Maurel and Thalmann, 1999	Ellipsoid	
		El Habachi et al., 2015	Ellipsoid	x
		Quental et al., 2012	Ellipsoid	
		Karlsson and Peterson, 1992	Ellipsoid	
		Dubowsky et al., 2008	Ellipsoid	
		Prinold and Bull, 2014	Ellipsoid	x
		Berthonnaud et al., 2006	Cone	
	Gliding plane	van der Helm, 1994a		
		Blana et al., 2008		
		Garner and Pandy, 1999		
		Tondu, 2007		
	Parallel mechanism	Ingram et al., 2016		
	Coupling equations	Sholukha et al., 2013		x
		Seth et al., 2016		x
		Holzbaur et al., 2005		
		Dickerson et al., 2007		
		Saul et al., 2015		

Notes: GH = glenohumeral joint, AC = acromioclavicular joint, SC = sternoclavicular joint, ST = scapulathoracic joint, DoF = degrees of freedom.

19

Table 2: Joint models of the forearm (the MBO column indicates whether the model was initially built for multibody kinematic optimisation purposes)

Joints	Kinematics	References	Comments	MBO
Elbow joint (merged HU and HR joints)	Universal joint	Prokopenko et al., 2001 Cerveri et al., 2003 Debril et al., 2011 Fohanno et al., 2013	Ulna and radius as a single segment Allow pronosupination	x x x x
HU joint	Hinge joint	Lemay and Crago, 1996 Pennestrì et al., 2007 Laitenberger et al., 2014		 x
HR joint	Spherical joint	Fick, 2013 Lemay and Crago, 1996 Pennestrì et al., 2007 Weinberg et al., 2000 Laitenberger et al., 2014	No pronosupination	 x
Wrist joint (merged RU and RC joints)	Universal joint	Prokopenko et al., 2001 Cerveri et al., 2003 Debril et al., 2011 Fohanno et al., 2013	Ulna and radius as a single segment	x x x x
RU joint	Spherical joint (distal RU joint)	Fick, 2013		
	Cylindrical joint (distal RU joint)	Lemay and Crago, 1996		
	Guide joint (proximal RU joint) + Spherical joint (distal RU joint)	Pennestrì et al., 2007		
	{Spherical joint + Prismatic joint} (proximal RU joint) + Hinge joint (distal RU joint)	Weinberg et al., 2000		
	{Hinge joint + Prismatic joint} (proximal RU joint) + 3 Hinge joints (distal RU joint)	Laitenberger et al., 2014		x
RC joint	Universal joint	Lemay and Crago, 1996 Weinberg et al., 2000 Laitenberger et al., 2014		 x
	Spherical joint	Pennestrì et al., 2007		

Notes: HU = humeroulnar joint, HR = humeroradial joint, RU = radioulnar joint, RC = radiocarpal joint, DoF = degrees of freedom.